

# Top-down and bottom-up inventory approach for above ground forest biomass and carbon monitoring in REDD framework using multi-resolution satellite data

Laxmi Kant Sharma · Mahendra Singh Nathawat · Suman Sinha

Received: 6 February 2012 / Accepted: 4 April 2013 / Published online: 20 April 2013  
© Springer Science+Business Media Dordrecht 2013

**Abstract** This study deals with the future scope of REDD (Reduced Emissions from Deforestation and forest Degradation) and REDD+ regimes for measuring and monitoring the current state and dynamics of carbon stocks over time with integrated geospatial and field-based biomass inventory approach. Multi-temporal and multi-resolution geospatial synergic approach incorporating satellite sensors from moderate to high resolution with stratified random sampling design is used. The inventory process involves a continuous forest inventory to facilitate the quantification of possible CO<sub>2</sub> reductions over time using statistical up-scaling procedures on various levels. The combined approach was applied on a regional scale taking Himachal Pradesh (India), as a case study, with a

hierarchy of forest strata representing the forest structure found in India. Biophysical modeling implemented revealed power regression model as the best fit ( $R^2=0.82$ ) to model the relationship between Normalized Difference Vegetation Index and biomass which was further implemented to calculate multi-temporal above ground biomass and carbon sequestration. The calculated value of net carbon sequestered by the forests totaled to 11.52 million tons (Mt) over the period of 20 years at the rate of 0.58 Mt per year since 1990 while CO<sub>2</sub> equivalent reduced from the environment by the forests under study during 20 years comes to 42.26 Mt in the study area.

**Keywords** Geospatial · REDD/REDD+ · Biomass inventory · Carbon · MODIS · NDVI

---

L. K. Sharma (✉)  
Centre for Land Resource Management, Central University  
of Jharkhand, Ranchi, Jharkhand, India  
e-mail: laxmikant1000@yahoo.com

L. K. Sharma  
e-mail: lksharma@bitmesra.ac.in

M. S. Nathawat  
School of Sciences, Indira Gandhi National Open  
University (IGNOU), New Delhi, India  
e-mail: msnathawat@ignou.ac.in

S. Sinha  
Department of Remote Sensing, Birla Institute of  
Technology, Mesra, Ranchi, Jharkhand, India  
e-mail: sumanrupa.sinha@gmail.com

## Introduction

Forests are a natural thwart on climate change as these sequester maximum carbon in their biomass. Deforestation of tropical forests released carbon of nearly 1–2 billion tons annually during the 1990s, roughly 15%–25% of annual global greenhouse gas emissions (Malhi and Grace 2000; Fearnside and Laurance 2003, 2004; Houghton 2005; Canadell et al. 2007; van der Werf et al. 2009). The reduction in these emissions can serve as a way to solve or reduce the climate change problem. Deforestation and forest degradation act as the main

source of emissions of greenhouse gases (GHGs) in most tropical countries. As estimated by the Intergovernmental Panel on Climate Change (IPCC), an annual total of 1.6 billion tons of carbon is released worldwide by land-use change activities, of which a major part results from deforestation and forest degradation (FAO 2005; Denman et al. 2007). Simultaneously, deforestation of tropical forests destroys carbon sinks that sequester CO<sub>2</sub> from the atmosphere and are vital for future climate stabilization (Stephens et al. 2007). The United Nations Framework Convention on Climate Change (UNFCCC) recently adopted an initiative step to provide financial incentives to facilitate reductions in emissions from deforestation below a baseline in developing countries, i.e., REDD (Reduced Emissions from Deforestation and forest Degradation) (Gibbs et al. 2007).

The concept of REDD is derived from RED (Reduced Emissions from Deforestation) and further concepts of REDD+ and REDD++/REALU (Reducing Emissions from All Land Uses) are presently originating out of REDD which reveals the importance and severity of the concept on a global scale. REDD+ comprises conservation, sustainable management of forests, and enhancement of forest carbon stocks, in addition to the concept of REDD. REALU, on the other hand, considers the emissions not only from forests but for all land uses. The basic steps required for successful implementation of a viable REDD regime include the assessment of forest carbon stocks and their change over time; quantifying the amount of reduced CO<sub>2</sub> emissions, which qualifies for accounting; identifying and ranking of the relevant causes for human impact on forests (Sinha et al. 2012) in order to derive effective measures to combat the degradation of forests; defining a baseline against which the changes of carbon stocks in forests are set off; and finally implementing a scheme for the transfer of benefits to local actors (Plugge et al. 2010).

The intention of the Kyoto Protocol is to limit or reduce CO<sub>2</sub> and other GHGs by an average value of 5 % of 1990 levels in the commitment period 2008–2012 (UNFCCC 1998). The United Nations Collaborative Program on Reducing Emissions from Deforestation and Forest Degradation in Developing Countries (UN-REDD Program) strategy for the period 2011–2015 targets to assist developing countries to build capacity to reduce emissions and to participate in a future REDD+ mechanism. India follows an inclusive approach to REDD which is termed as a REDD Plus approach that deals with compensating countries for “reducing deforestation”

along with “conservation, sustainable management of forest and increase in forest cover” (ICFRE 2007). UNFCCC (1998), India, with a view of CDM (Clean Development Mechanism), considers REDD as “Reducing Emissions from Deforestation in Developing countries”, Sustainable Forest Management (SFM), and Afforestation and Reforestation (A&R), which reveals the comprehensive approach (MoEF 2009). India has strong forest monitoring capacities, with several satellites launched that provide medium resolution imagery suitable for monitoring forest cover change. Accurate delineation of successional and mature forest biomass distribution becomes considerably significant in reducing the uncertainty of carbon emission and sequestration.

Owing to the dynamism of nature, the land use land cover features changes with time (Sharma et al. 2012). Changes in forest cover at regional to global level requires remote-sensing-based approaches, though for small aerial extent, it can be assessed through field-based techniques (Trigg et al. 2006). Among all the land-use systems involving trees, the most significant carbon pool preserved as Above Ground Biomass (AGB) (Ravindranath and Ostwald 2008) is susceptible to frequent changes which require recurrent monitoring. According to Biomass ECV report (2009), the techniques involved in biomass estimation are destructive sampling, non-destructive sampling, remote sensing, and model-based techniques. Remotely sensed data with its synoptic view, high spatio-temporal resolution, and digital format allows fast processing of large quantity of data as well as the availability of data for that particular area of forest which is inaccessible by field survey. Optical remote sensing mainly responds to the leaf chemistry or structure to measure the vegetation indices like normalized difference vegetation index (NDVI) and uses the technique of modeling based on NDVI–biomass relations to estimate the aboveground biomass of the whole forest area (Dong et al. 2003). Baccini et al. (2004) made use of MODIS (Moderate Resolution Imaging Spectroradiometer) data to estimate biomass over regional scales along with other multi-source data. Lu (2006) has given a brief description of several research works completed with different approach methods and models applied through optical sensor data of different spatio-resolution for AGB and forest stand parameter estimation.

Assessment of AGB for moist tropical forests is difficult and challenging because of its complicated and abundant stand structure and varied species

composition using spectral responses (Lucas et al. 1998; Nelson et al. 2000; Steininger 2000; Foody et al. 2001, 2003) in comparison to coniferous forests. AGB can be directly estimated using remotely sensed data with different approaches like multiple regression analysis, K nearest neighbor, and neural network (Roy and Ravan 1996; Nelson et al. 2000; Steininger 2000; Foody et al. 2003; Zheng et al. 2004) and indirectly estimated from canopy parameters, such as crown diameter, which are first derived from remote sensed data using multiple regression analysis or different canopy reflectance models (Woodcock et al. 1997; Phua and Saito 2003; Popescu et al. 2003). Tropical AGB estimation has been investigated with Landsat TM (Sader et al. 1989; Lucas et al. 1998; Boyd et al. 1999; Nelson et al. 2000; Steininger 2000; Foody et al. 2001, 2003; Lu 2005) or synthetic aperture radar (SAR) data (Rignot et al. 1995; Luckman et al. 1997, 1998; Santos et al. 2002, 2003), but the studies show difficulty in AGB estimation based on purely spectral responses from optical sensor data or backscatters from SAR data. Studies have shown that textures are also helpful in improving land cover or vegetation classification (Franklin and Peddle 1989; Marceau et al. 1990; Augusteijn et al. 1995; Podest and Saatchi 2002).

## Methodology

### Study area

Himachal Pradesh covers a total area of 55,673 km<sup>2</sup> with the geographic extent of 30°22' to 33°12' N latitude and 75°45' to 79°04' E longitude (Fig. 1); the altitude varies from 350 m to 6,975 m above the mean sea level. The state has three distinct regions: Shiwaliks (altitudes up to 1,500 m), Middle Himalayan region (1,500–3,000 m altitude), and the Himadris (>3,000 m altitude). Tree growth is minimal and is governed by elevation and precipitation. Nearly one third of the geographical area is permanently under snow and glaciers while remaining under recorded forests covering an area of 37,033 km<sup>2</sup> (Forest Survey of India 2009). Reserved Forests constitute 5.13 %, Protected Forests 89.27 %, and Unclassed Forests 5.60 % of the total forest area of Himachal Pradesh. The state has 35 different forest

types (Champion and Seth 1968) divided into eight groups, namely, Tropical Moist Deciduous, Tropical Dry Deciduous, Subtropical Pine, Himalayan Moist Temperate, Himalayan Dry Temperate, Sub Alpine Forests, Moist Alpine Scrub, and Dry Alpine Scrub.

### Area zonation

The complete methodology adopted in the study is presented in Fig. 2. MODIS with spatial resolution of 250 m was used for zoning of the total land area under study. Broad forest classes related to AGB calculation are based on stratification rules (GPG–LULUCF; IPCC 2003). Pre-processing was not done for the cloud-free 16-day composite MOD13Q NDVI products as standard scientific product made available by NASA to meet the needs of the research. The VI (Vegetation Index) products are validated with accuracies depicted by a pixel reliability flag with globally averaged uncertainties of only 0.015 units. Knowledge-based Decision Tree image classification techniques were applied for MODIS-NDVI 250 m 16-day composite data over the years 2000, 2005, and 2010 for zoning of total land into forest and non-forest. MOD13Q NDVI products were in Geographic Coordinate System and converted to UTM Zone 43 North before any further analysis using MRT (MODIS Reprojection Tool, version 4.0) and the area of interest subsetted using ERDAS Imagine. In context to REDD, a combined inventory aims to focus mainly on forest areas that show ample changes in their spatial extent (Plugge et al. 2010). Knowledge-based Decision Tree algorithm was considered better for classification as this surpassed the Maximum Likelihood classification approach (Chen and Rao 2009). This classification technique also integrated SRTM (Shuttle Radar Topographic Mission) DEM and climate data (rain-fall data) for the region. This algorithm was based on predecided reconnaissance knowledge-based criteria set up for the particular analysis, hence had better potential. The Knowledge Classification application is the means by which knowledge bases constructed with the Knowledge Engineer, the dialog where all of the main functions for creating and testing a knowledge base are accessible, were processed. The classes and input data required for a particular analysis were selected for existing knowledge base to be used for classification. The following criteria were considered for identification:

**Fig. 1** Study area

- The assessment area should represent the entire target region.
- Derived results should be transferable to other areas of the state with similar characteristics.
- The assessment area should exhibit diverse intensities of forest degradation.
- Other criteria like infrastructure, accessibility, and funding were also considered.

#### Pre-processing and image rectification

High-resolution multispectral Landsat-5 TM and IRS P-6 LISS-III data were rectified and utilized to stratify and form similar forest type clusters within the assessment areas. Consecutive two time (archive and present) data were used for analyzing change detection of both forest area and carbon stock. Landsat-5 TM imagery for the year 1990 were downloaded from the website [www.landsat.org](http://www.landsat.org) with minimum cloud cover to avoid the seasonal variation in the vegetation phenology, the details of which are documented in Table 1. As observed through visual interpretation, the elevated areas had shadow effect and dark pixel problem. Dark Object Subtraction (DOS), haze reduction, and conversion of DN to top of atmosphere reflectance were executed as a

part of radiometric correction along with image-based COST method for atmospheric correction. Chavez (1996) improved dark-object atmospheric correction for bands 1–5, and 7 of Landsat-5 TM multispectral data was implemented. The steps for calculating reflectance ( $\rho$ ) from the fundamental radiance considering the haze correction is given in Eqs. 1 to 4 (Chavez 1996).

$$L_{\lambda, \min} = L_{\text{MIN}\lambda} + \text{QCAL} * (L_{\text{MAX}\lambda} - L_{\text{MIN}\lambda}) / \text{QCALMAX} \quad (1)$$

where QCAL is the minimum DN, QCALMAX=255, and constants  $L_{\text{MIN}\lambda}$ ,  $L_{\text{MAX}\lambda}$  are given in the table of Markham and Barker (1986).

$$L_{\lambda, 1\%} = 0.01 * d^2 * \cos^2\theta / (\pi * \text{ESUN}\lambda) \quad (2)$$

where  $\text{ESUN}\lambda$ =mean solar exoatmospheric spectral irradiance from Markham and Barker (1986),  $d$  is the Sun–Earth distance, and  $\theta$  is the solar zenith angle (90–sun elev.).

$$L_{\lambda, \text{haze}} = L_{\lambda, \min} - L_{\lambda, 1\%} \quad (3)$$

$$\rho = \pi * d^2 * (L_{\lambda, \text{sat}} - L_{\lambda, \text{haze}}) / \text{ESUN}\lambda * \cos^2\theta \quad (4)$$

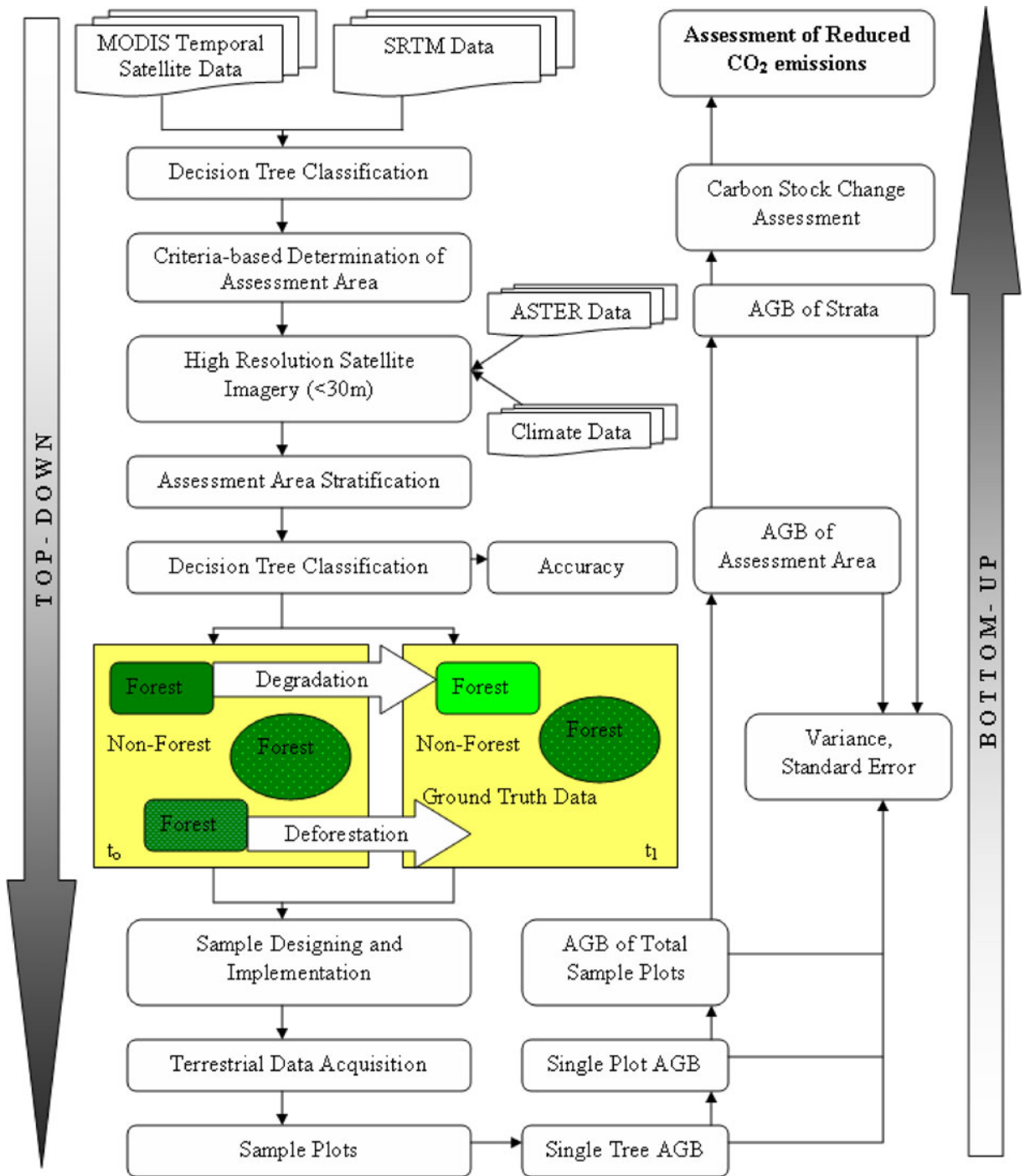


Fig. 2 Methodology for quantifying reduced CO<sub>2</sub> emission

Though the output from the model should range from 0 to 1, however, values greater than 1 corresponding to

bright objects (e.g., clouds, snow, and playa) or noise are obtained.  $L_{haze}$  values for each band was calculated

**Table 1** Satellite data acquisition details

S. no.	Satellite/sensor	Path/row	Date of acquisition	Time of acquisition
1	Landsat-5 TM	146/037	18-10-1989	04:35:00.0 pm
2	Landsat-5 TM	146/038	21-10-1990	04:35:00.0 pm
3	Landsat-5 TM	146/039	21-10-1990	04:36:00.0 pm
4	Landsat-5 TM	147/037	09-10-1989	04:35:00.0 pm
5	Landsat-5 TM	147/038	09-10-1989	04:35:00.0 pm
6	Landsat-5 TM	147/039	25-10-1989	04:36:00.0 pm
7	Landsat-5 TM	148/037	04-07-1992	04:35:00.0 pm
8	Landsat-5 TM	148/038	16-10-1989	04:35:00.0 pm
9	IRS-P6 LISS-III	094/047	14-09-2009	05:50:49.0 pm
10	IRS-P6 LISS-III	094/048	12-05-2010	05:50:32.0 pm
11	IRS-P6 LISS-III	094/049	12-06-2010	05:50:53.0 pm
12	IRS-P6 LISS-III	095/047	13-10-2009	05:46:43.0 pm
13	IRS-P6 LISS-III	095/048	13-10-2009	05:47:04.0 pm
14	IRS-P6 LISS-III	095/049	13-10-2009	05:47:24.0 pm
15	IRS-P6 LISS-III	096/048	09-07-2010	05:41:36.0 pm
16	IRS-P6 LISS-III	096/049	22-05-2010	05:42:25.0 pm
17	IRS-P6 LISS-III	097/049	27-05-2010	05:38:11.0 pm

using Table 2 which further served as an input to Chavez's COST model as shown in Fig. 3. The general equation is given below:

$$\frac{((-L_{\text{haze}} + (a * \text{Image Band } i) - b) * \pi * d^2)}{(c * \cos(\pi/180 * (90 - \text{sun elev.}))^2)} \quad (5)$$

where  $a$ ,  $b$ , and  $c$  are band-specific constants.

IRS P-6 LISS-III imagery (Table 1) were procured from NRSC, Hyderabad with minimum cloud cover of

the same season to avoid seasonal variation. Similar radiometric corrections were performed as of Landsat-5 TM imagery. For this purpose, the at-surface reflectance is calculated with the following formula (Sobrino et al. 2004):

$$\rho = \frac{\pi(L_{\text{sat}} - L_p)d^2}{E_0 \cos \theta_z T_z} \quad (6)$$

where  $L_{\text{sat}}$  is the at-sensor radiance,  $T_z$  is the atmospheric transmissivity between the sun and the surface,  $\theta_z$  is the zenithal solar angle,  $d$  is the Earth–Sun

**Table 2**  $L_{\text{haze}}$  calculation for satellite data

Band	DN <sub>min</sub>	S. elev.	1 %	HL <sub>min</sub>	L1%	$L_{\text{haze}}$	$(L_{\text{max}} - L_{\text{min}})/255$	$L_{\text{min}}$	$L_{\text{max}}$	S–E dist.	S. exo.
TM-1	30	40	0.01	1.6570588	0.2594521	1.3976067	0.0602353	−0.15	15.21	0.9960000	195.7
TM-2	10	40	0.01	0.8949020	0.2424824	0.6524196	0.1174902	−0.28	29.68	0.9960000	182.9
TM-3	8	40	0.01	0.5247059	0.2064216	0.3182843	0.0805882	−0.12	20.43	0.9960000	155.7
TM-4	5	40	0.01	0.2572549	0.1388076	0.1184473	0.0814510	−0.15	20.62	0.9960000	104.7
TM-5	2	40	0.01	−0.0153843	0.0290740	−0.0444583	0.0108078	−0.037	2.719	0.9960000	21.93
TM-7	2	40	0.01	−0.0036039	0.0098796	−0.0134835	0.0056980	−0.015	1.438	0.9960000	7.452
LISS-2	38	15.98	0.01	1.7977725	0.0434982	1.7542743	0.0473098	0	12.064	1.0102000	184
LISS-3	20	15.98	0.01	1.1867451	0.0366425	1.1501026	0.0593373	0	15.131	1.0102000	155
LISS-4	15	15.98	0.01	0.9268824	0.0252952	0.9015872	0.0617922	0	15.757	1.0102000	107
LISS-5	9	15.98	0.01	0.1198941	0.0054373	0.1144568	0.0133216	0	3.397	1.0102000	23

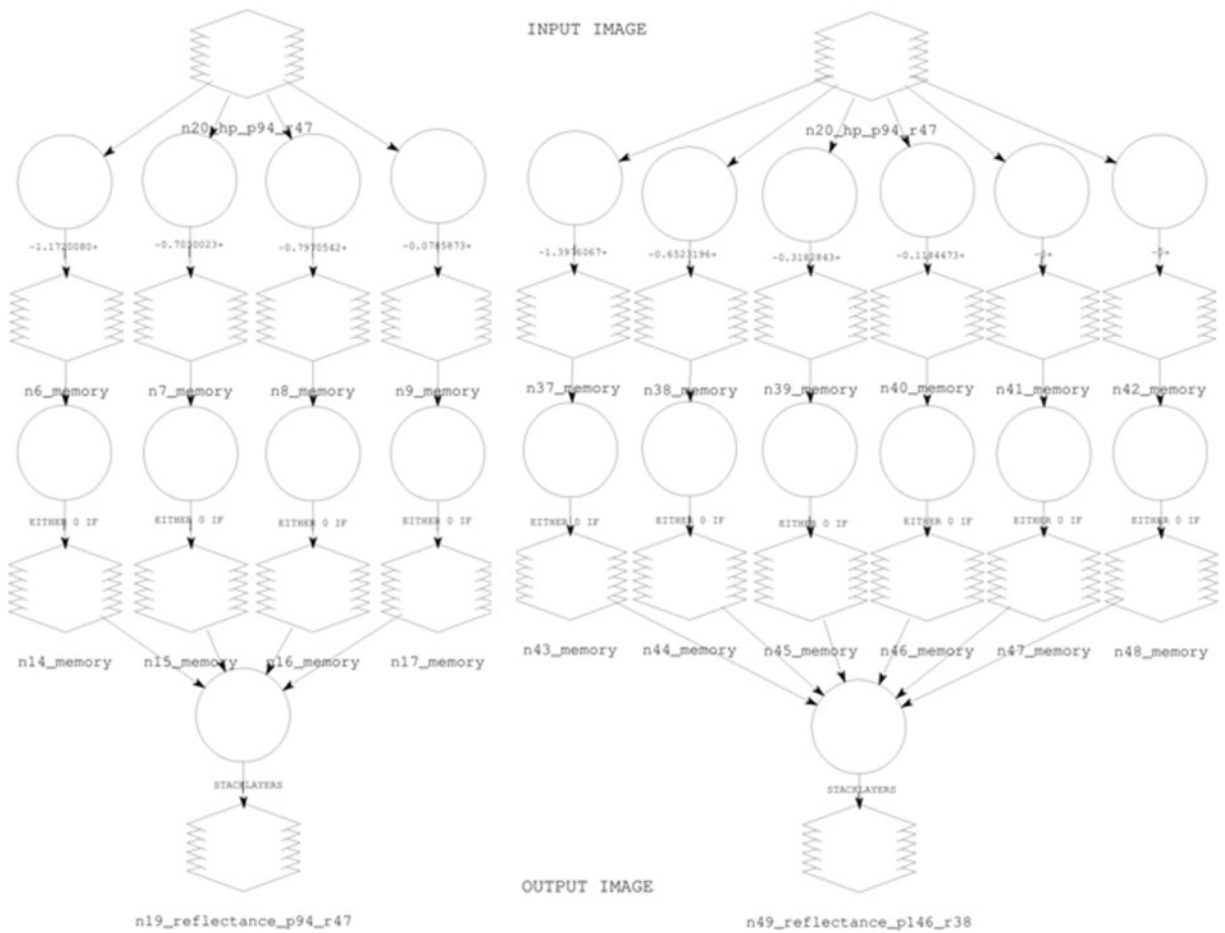


**Fig. 3** Chavez’s COST model for data processing

distance, and  $L_p$  is the radiance resulted from the interaction of the electromagnetic radiance with the atmospheric components (molecules and aerosols) that can be obtained with the below given equation:

$$L_p = L_{min} - L_{1\%} \tag{7}$$

where  $L_{1\%} = \frac{0.01 \cos \theta_z T_z E_0^1}{\pi d^2}$  and  $\tag{8}$

$$T_z = \cos \theta_z \tag{9}$$

$$L_{sat} = \frac{L_{max} - L_{min}}{255} * DN + L_{min} \tag{10}$$

where  $L_{max}$  and  $L_{min}$  ( $mw/cm^2.sr.\mu m$ ) are the maximum and minimum spectral radiance, respectively.

The Earth–Sun distance “ $d$ ” was computed using the equation (Van 1996):

$$d = 1 + 0.0167 \sin[2\pi(D - 93.5)/365] \tag{11}$$

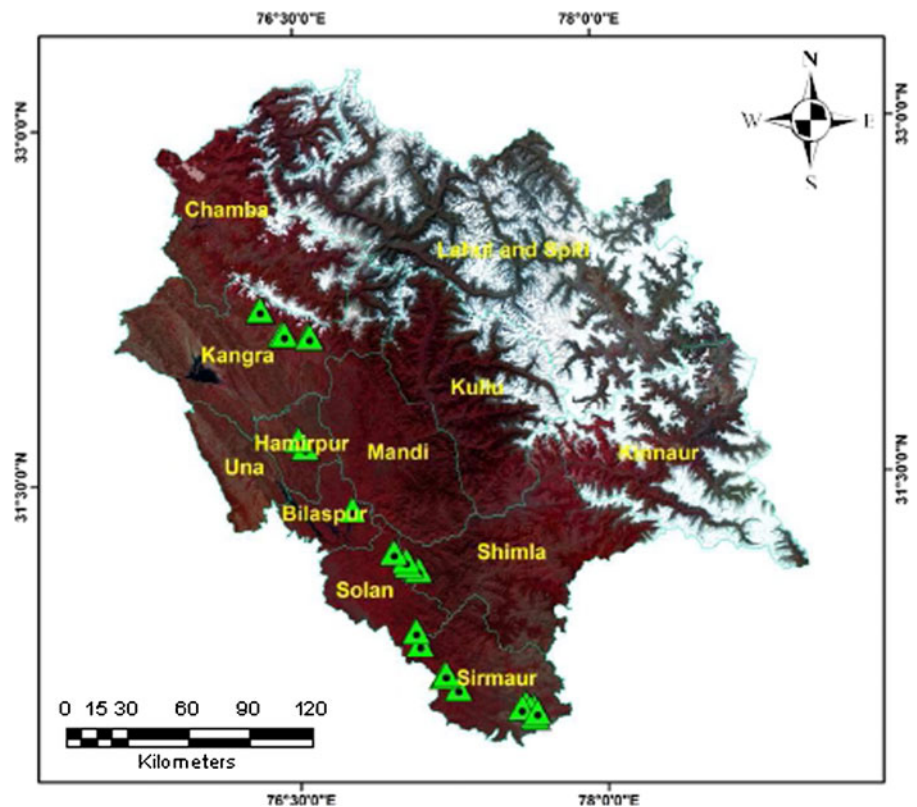
For LISS-III data, the spectral solar irradiance on top of the atmosphere,  $E_0$  and  $E_0^1$  for bands 2, 3, 4, and 5 are 185.22, 157.73, 109.67, and 24.06 and 184, 155, 107, and 23, respectively (Pandya et al. 2002).

All the scenes of Landsat-5 TM and LISS III obtained after processing through the Chavez’s COST model (Eq. 5) with different values for the constants  $a$ ,  $b$ , and  $c$  were mosaicked and the area of interest subsetting in ERDAS Imagine.

### Image classification

NDVI calculated from the images were used as inputs for knowledge-based decision tree image classification.

**Fig. 4** GPS sample plot location



Landsat-5 TM (NDVI), IRS P-6 LISS-III (NDVI), ASTER DEM, and Slope Map based on ASTER DEM all co-registered. The six land use classes viz. Forest Land, Crop Land, Grass Land, Wetlands, Settlements, and Other Lands as per GPG–LULUCF from two classified maps of two time periods were derived. Further, based on the same knowledge-based principle, the forest area

from both time periods were converted into strata of forest depending on the different climatic (IPCC 2006) and elevation (H.P. Forest department) zones for field inventory. Threshold values for NDVI, climate (rainfall), climatic zones, and elevation zones were derived after consulting different published materials, literatures, direct field information, and Google Earth. Classified data often

**Table 3** Local tree volume equations (Himachal Pradesh)

S. no.	Forest tree species	Volume equation	WD <sup>a</sup> (tons dry matter/m <sup>3</sup> )	BEF <sup>b</sup> (biomass expansion factor)
1	<i>Shorea robusta</i>	$0.1919 - 2.7070 * D + 11.7563 * D^2$	0.72	1
2	<i>Pinus roxburghii</i>	$0.2283 - 1.7288 * D + 9.05 * D^2$	0.65	0.95
3	<i>Quercus dilatata</i>	$0.0988 - 1.5547 * D + 10.1631 * D^2$	0.7	4.2
4	<i>Pinus wallichiana</i>	$0.291006 - 3.54227 * D + 16.894379 * D^2$	0.48	0.81
5	<i>Cedrus deodara</i>	$0.167174 - 1.735312 * D + 12.039017 * D^2$	0.56	0.81
6	<i>Quercus semecarpifolia</i>	$0.13581 - 1.84908 * D + 10.82341 * D^2$	0.58	1.4
7	<i>Quercus incana</i>	$(0.240157 + 3.820069 * D - 1.394520 * \sqrt{D})^2$	0.7	3.4

Source: Volume Equations for Forests of India, Nepal and Bhutan–FSI

<sup>a</sup>WD from Sharma et al. 2008 and IPCC 2006

<sup>b</sup>BEF from Chhabra et al. 2002



manifest a salt-and-pepper appearance due to the inherent spectral variability encountered by a classifier when applied on a pixel-by-pixel basis (Lillesand et al. 2007). Hence, the classified images were smoothed with  $3 \times 3$  majority filter.

**In situ assessment**

Data for the land use and forestry obtained from sample surveys were used to assess land use and carbon stock changes. The stratified random sampling method was employed as sampling efficiency enhances due to stratification as subdivision of the population reduces the variability between units within a stratum as compared to the variability within the entire population. Sampling quadrats of regular shape of dimensions  $10 \times 10$  m,  $5 \times 5$  m, and  $1 \times 1$  m, nested within each other, were

defined as the units for sampling (Hernandez et al. 2004). The number of sampling units is calculated as (Chacko 1965):

$$N = \frac{t^2 * (CV)^2}{(SE\%)^2} \tag{12}$$

where  $N$ =number of sample plot,  $CV$  = coefficient of variation,  $SE$  = standard error percentage (10 %), and  $t$  = statistical value at 95 % significance level.

Sample plot location was captured using geodetic Trimble GPS in the field and imported in ArcGIS framework to generate the location map of the sample plots (Fig. 4). Several dendrometric data such as DBH (diameter at breast height), total height, and crown parameters as well as ancillary data related to the structure and status of forest, forest type and density,

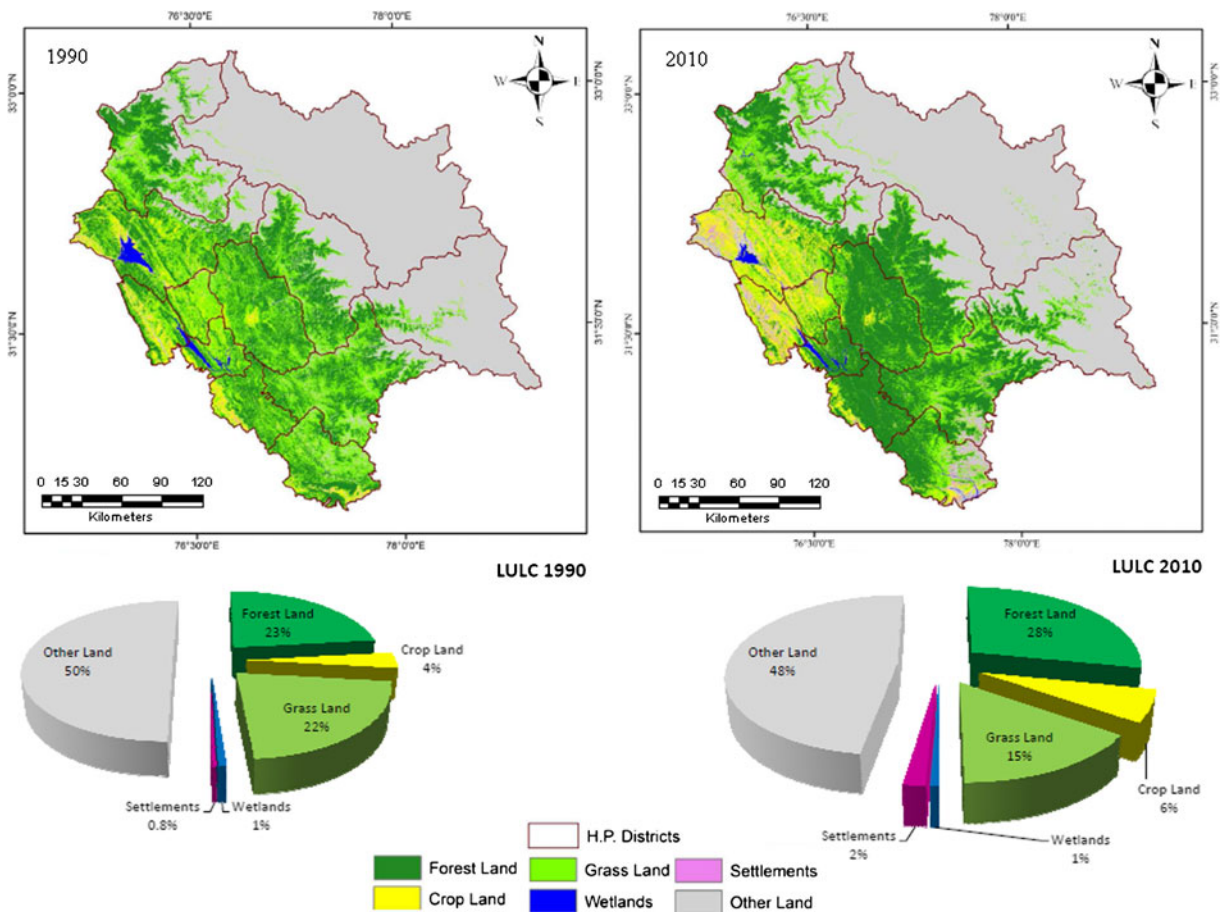


**Fig. 5** Land use and land cover (1990 and 2010)

**Table 4** Forest area (Himachal Pradesh)

Forest zones	Area in hectares			
	Year 1990	Year 2000	Year 2005	Year 2010
Tropical Forests	372,491.76	469,706.25	545,906.25	620,537.5
Montane Sub-Tropical Forests	351,853.79	367,575	410,993.75	558,862.5
Montane Temperate Forests	445,483.88	403,400	403,462.5	359,012.5
Alpine Forests	122,080.77	67,962.5	67,962.5	61,225
Total Forest	1,291,910.2	1,308,643.75	1,428,325	1,599,637.5
Non-Forest	4,311,327.3	4,294,593.75	4,174,912.5	4,003,600

sample plot location, and its topographic characteristic including possible human-induced impacts were also collected.

#### AGB calculation

Volume of each tree was enumerated using species-specific local volume equations formulated by Forest Survey of India (Table 3). The AGB of a single tree (AGB<sub>tree</sub>) was calculated as:

$$AGB_{tree} = V * WD * BEF \quad (13)$$

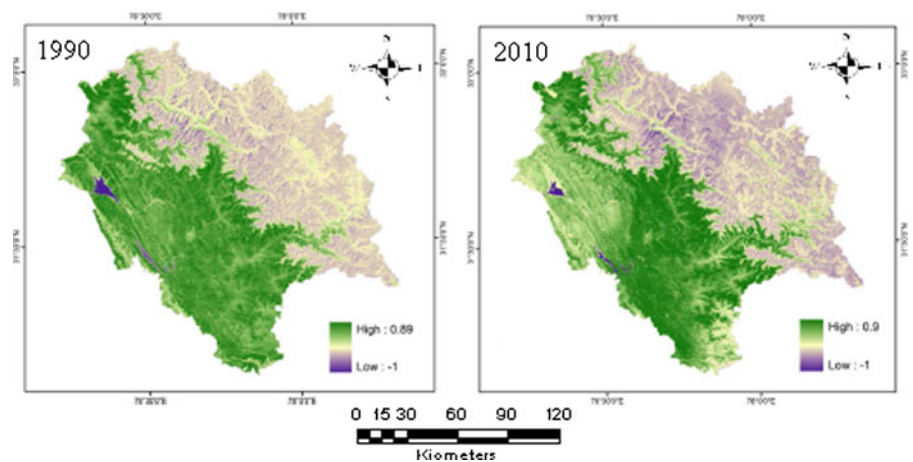
where  $V$  = merchantable volume ( $m^3$ ),  $WD$  = species-specific wood density (tons dry matter/ $m^3$ ), and  $BEF$  = species- and site-specific biomass expansion factor

The species-specific wood density (Sharma et al. 2008; IPCC 2006) and site-specific biomass expansion factor (BEF) (Chhabra et al. 2002) were adopted from existing literature (Brown et al. 1989; IPCC 2006). In case of data unavailability, default values

for tropical hard or softwoods (IPCC 2006) were applied. Default values provided by IPCC (2006) were used to convert biomass into carbon. Up-scaling procedures expand sample plot data to area related estimates (e.g., strata, state, or country) resulting in aggregation of respective AGB values on different scales (Riedel 2008).

#### CO<sub>2</sub> emissions

The proportion of carbon in tree biomass varies more between different tree compartments than between the tree species (Wirth et al. 2002; Mund et al. 2002; Schulze 2000). On tree level, the proportion of branch and leaf biomass to the stem biomass is higher in younger age classes (Hakkila 1989). The average carbon concentration of  $0.47 \text{ g C g}^{-1}$  of dry weight in tree biomass has been implemented for all test sites (Wirth et al. 2004; IPCC 2006). Quantification of reduced CO<sub>2</sub> includes a reference level for enumerating changes of carbon stocks in forests and a continuous

**Fig. 6** NDVI map (1990 and 2010)

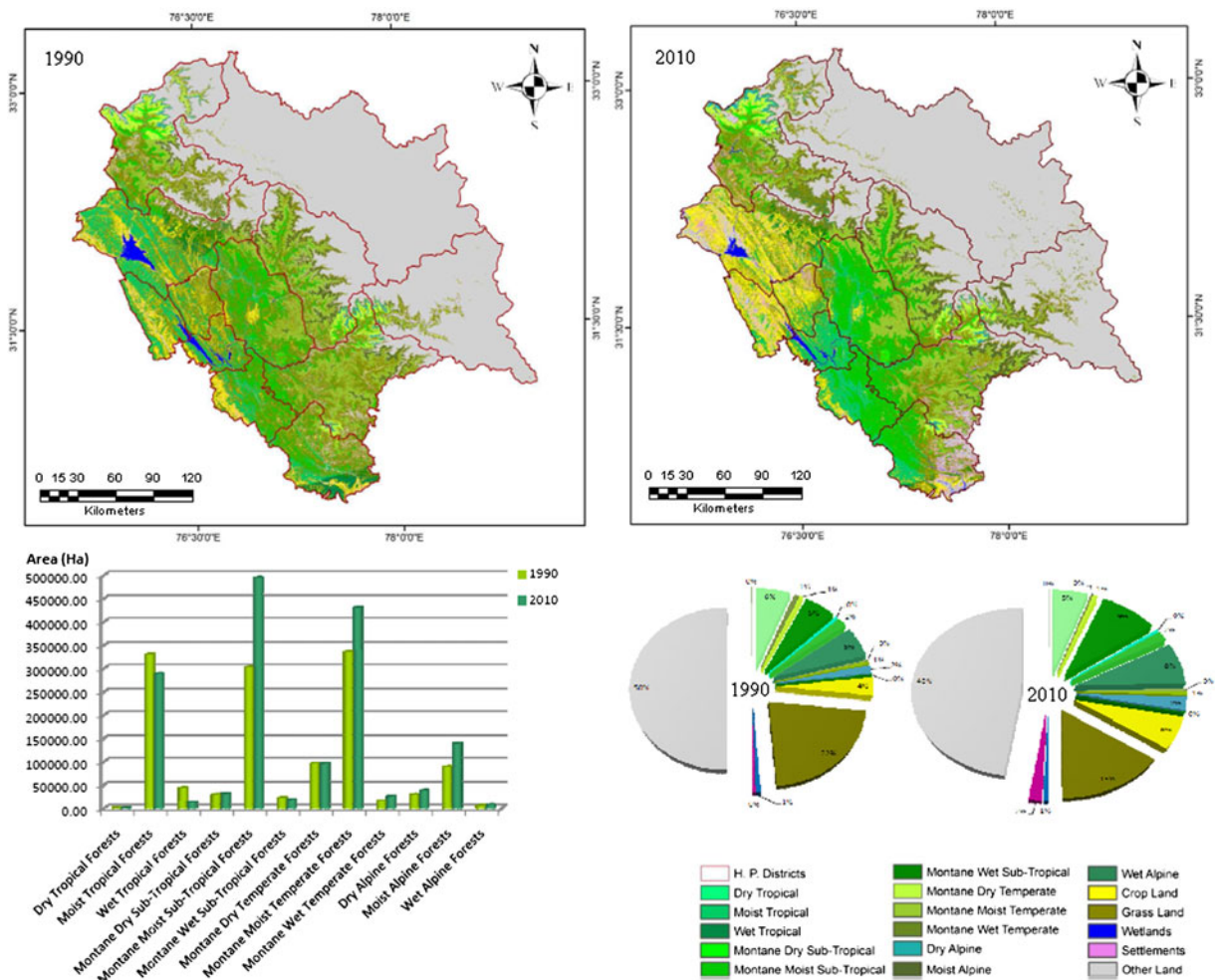


**Fig. 7** Forest strata statistics (1990 and 2010)

**Table 5** Stratified forest cover change and AGB calculation

Strata	Area in hectares			AGB (t/ha)	AGB (t)
	1990	2010	Change		
Dry Tropical Forests	398.90	243.07	-155.82	60	-9,349.44
Moist Tropical Forests	329,338.46	287,944.01	-41,394.45	182	-7,533,789.19
Wet Tropical Forests	42,754.40	12,338.84	-30,415.56	275	-8,364,279.45
Montane Dry Sub-Tropical Forests	28,543.36	30,508.36	1,965.00	50	98,250.00
Montane Moist Sub-Tropical Forests	302,063.51	493,729.63	191,666.12	127	24,341,597.49
Montane Wet Sub-Tropical Forests	21,246.92	17,574.28	-3,672.64	222	-815,325.71
Montane Dry Temperate Forests	95,773.21	95,555.92	-217.29	122	-26,508.96
Montane Moist Temperate Forests	334,740.25	429,992.12	95,251.88	128	12,192,240.04
Montane Wet Temperate Forests	14,970.42	25,120.80	10,150.38	134	1,360,151.28
Dry Alpine Forests	28,530.69	37,032.83	8,502.14	20	170,042.76
Moist Alpine Forests	88,158.77	138,646.89	50,488.11	60	3,029,286.86
Wet Alpine Forests	5,391.31	7,014.47	1,623.16	50	81,158.05

monitoring of the same. The following formula was used for calculating reduced equivalent CO<sub>2</sub> at two time intervals  $t_1$  and  $t_2$  (IPCC 2006):

$$\text{Reduced CO}_2 = \frac{(C_{t_2} - C_{t_1}) * 44}{12} \quad (14)$$

## Results and discussions

### LULC Classification

The result obtained from knowledge-based expert classification using decision tree algorithm was better than other classification techniques for such a large area and showed consistent results. The inputs to the expert classifier were in the form of NDVI images for the two time periods (1990 and 2010), ASTER DEM and slope map generated using ASTER DEM. Results show that the land use land cover areal coverage changed dynamically in the span of 20 years (Fig. 5). The spatial extent of different classes of land use in 1990 and 2010 can be accessed from the LULC map shown in Fig. 5 with an overall accuracy of 81.50 % and 88.75 % and Kappa accuracy of 0.77 and 0.85, respectively. Most of the area of upper Himalayas in the state remains snow covered and are deprived of vegetation.

### Temporal forest cover dynamics

Preliminary investigation of LULC classification and multi-temporal MODIS NDVI for the years 2000, 2005, and 2010 using knowledge-based expert classifier suggested a gain of forest cover from 1.3 Mha in 1990 to 1.6 Mha in 2010 (Table 4). Increment in total forest cover for over the first 5 years (2000–2005) was off 2 % while in the second 5 years (2005–2010) it was 4 %. This increase may be attributed to the new Indian Forest Policy of 1988 and good management practices of the Himachal Pradesh State Forest Department. MODIS indicated the continued areal increment of the Tropical forest zone and the Montane Subtropical forest zone since 2000 (Table 4). But within the same time period, Montane Temperate Zone and Alpine Zone had shown a decrease in their coverage especially in the duration 2005 to 2010; this may be due to some developmental activities in the region. The forest cover in Montane Temperate and Alpine Zone Zones remained

unchanged during 2000 to 2005 but decreased in 2010 owing to degradation and deforestation. Forest cover change dynamics as per MODIS data investigation suggests that there is increase in forest cover of Tropical zone in Himachal Pradesh during the period 2000 to 2010 while the Alpine Zone forest cover remained constant. Areal coverage remained constant for Montane Sub-Tropical forests from 2000 to 2005 but showed gradual increase of 3 % till 2010. Results suggest that the Himachal state is showing changes in coverage of forests which needs to be assessed. MODIS data are a coarse resolution (250 m) product and cannot be used for accurate forest area calculation and dynamics, so it was decided to use high-resolution (<30 m) Landsat-5 TM (1990) and IRS P-6 LISS-III (2010) data for recording of actual forest changes. The NDVI values varied from –1 to 0.89 in 1990 NDVI image and from –1 to 0.9 in 2010 NDVI image (Fig. 6). Biomass accumulation in the forest is a site-dependent phenomena, hence necessary for precise biomass assessment.

### Forest stratification

ASTER DEM, rainfall map, slope map based on ASTER DEM, and NDVI were used for the stratification. Twelve strata of forests were identified as per IPCC (2006) guidelines (Ravindranath and Ostwald 2008). During 1990–2010, the area showed degradation and deforestation in Tropical forests, either moist or dry (Table 5). Montane Dry Sub-Tropical and Montane Moist Sub-Tropical strata area were enhanced in the locality. Montane Wet Sub-Tropical strata of forests have shown area reduction because of deforestation and degradation. With a minor

**Table 6** Model statistics

S. no.	Model	R <sup>2</sup>	Standard error of prediction
1	Linear	0.735	68.390
2	Logarithmic	0.720	73.043
3	Inverse	0.698	73.043
4	Quadratic	0.741	68.814
5	Cubic	0.742	68.806
6	Compound	0.793	0.334
7	Power	0.815	0.315
8	Growth	0.793	0.334
9	Exponential	0.793	0.334

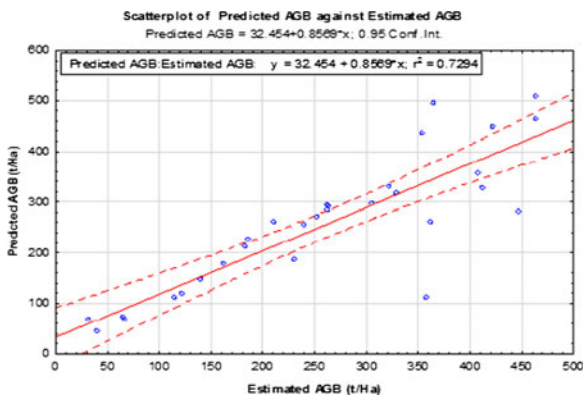


**Fig. 8** Scatterplot for estimated and predicted biomass

reduction in Montane Dry Temperate forests, Montane Moist and Montane Wet have increased in coverage during this time period of 20 years. All the strata (dry, moist, and wet) within Alpine Zone showed a net increment in their coverage area from 1990 to 2010, and the stratified forest map for 1990 and 2010 is shown in Fig. 7.

Temporal carbon stock dynamics

Dry, Moist, and Wet Tropical Forests depicted loss of forest cover over the period of 1990 and 2010 (Table 5). Nevertheless, Montane Wet Sub-Tropical Forests and Montane Dry Temperate Forests showed negative

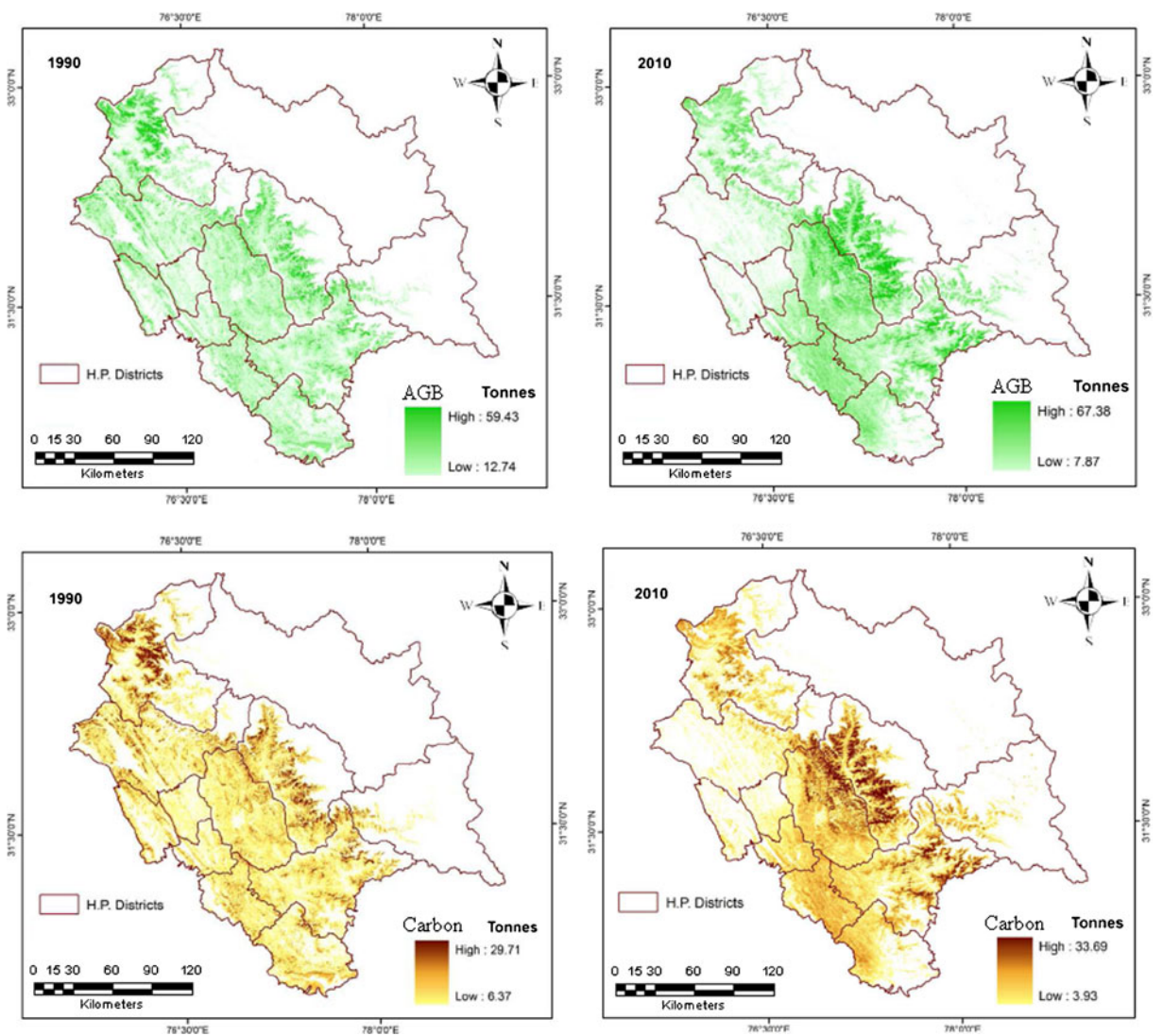


**Fig. 9** AGB and carbon maps for 1990 and 2010

change in forest cover within the same span of time while the remaining strata of forests showed a positive change in forest cover. Change of forest cover in Montane Moist Sub-Tropical Forests stratum is highest among all the forest strata. Wet alpine stratum showed least growth in forest cover within this period in the area. The forests demonstrated a net increase in AGB from 1990 to 2010 as quantified statistically and verified from remote sensing as well. The forest cover showed a net increase of ~0.28 Mha over the period of 20 years from 1990 to 2010 (Table 5). The table depicts a net increase in AGB, calculated to be 24.52 Mt at the rate of 12.3 Mt per annum. Modeling resulted in finding a best-fit line, correlation coefficient, and standard error of estimate (Table 6). The biomass calculated from sample plot data were plotted against NDVI extracted for the same location from NDVI of 2010 LISS-III image. Different models for curve estimation were applied in SPSS Statistics software to find a best-fit model which defines the relationship between NDVI and AGB. After analyzing the model values for  $r^2$  and “Standard Error of Prediction”, it was observed that the “Power model” best defines the relationship between NDVI and AGB as

$$\text{AGB} = 1169.8 * \text{NDVI}^{4.2043} \quad (15)$$

STATISTICA software was used to develop a scatter plot (Fig. 8) of estimated against predicted AGB values. At the 0.95 confidence level, predicted AGB showed high correlation ( $r^2=0.73$ ) with the field-based estimated AGB values. Maps showing relative abundance of AGB and forest carbon sequestration in the year 1990 and 2010 (Fig. 9) using Eq. 15 in ERDAS Imagine were prepared. The calculated value of the net Carbon sequestered by the forests totaled to 11.52 Mt over the period of 20 years in the study area at the rate of 0.58 Mt per year since 1990. During this 20 years, CO<sub>2</sub> equivalent reduced from the environment by the forests of the study area resulted to 42.26 Mt.

## Conclusions

Climate change has created prospects for deforestation within international pledge on emissions. Carbon enhancement activities and reduced emissions including both deforestation and forest degradation (REDD) should be considered of equal importance. Recognition of a REDD mechanism definitely has a staggered approach even though deforestation and degradation are

the instant precedence. The motivation behind this approach is mainly sensible for the political viability of negotiations under UNFCCC with a simpler scope and the need for building capacity in carbon accounting for developing countries. There is agreement for voluntary participation of only developing countries in REDD that includes economical incentives for reducing the emissions of GHGs. Articles 3.3 and 3.4 deal with the benefits of forests as carbon sinks (UNFCCC 1998) and afforestation and reforestation in CDM generate credits.

The methodology adopted in this study of carbon sequestration in the scope of REDD depends on the capacities in a country existing or which can be constructed. So by the end of the first commitment period, particular nations should have all the capacities in order to avoid the urgent need for broad-scale consultancy for which country-specific knowledge is essential. The applied methodology was designed using prior information about the study area and the forest cover distribution as published by Forest Survey of India, Dehradun and Himachal Pradesh State Forest Department, hence confirming the inclusion of site-specific knowledge. The challenge lies in the most effective synergism of multi-sensor geospatial and terrestrial inventories. This study reveals the potential of combined inventory and the statistical upscaling methods (top-down and bottom-up approaches) for producing consistent results on a national and/or sub-national level. For successive inventories in the scope of REDD, the in situ framework can be optimized for all of the adapted IPCC categories to fully exploit the advantages of a stratified random sampling design. The availability of cloudless very high resolution data can pose an immense challenge, especially in the Himalayan belt which can be possibly overcome by high resolution RADAR (e.g., Terra SAR-X, Cosmo-SkyMed, and ALOS PALSAR) and LIDAR data (Plugge et al. 2010).

## References

- Augusteijn, M. F., Clemens, L. E., & Shaw, K. A. (1995). Performance evaluation of texture measures for ground cover identification in satellite images of a neural network classifier. *IEEE Transactions on Geoscience and Remote Sensing*, 33, 616–625.

- Baccini, A., Friedl, A. M. A., Woodcock, C. E., & Warbington, R. (2004). Forest biomass estimation over regional scales using multisource data. *Geophysical Research Letters*, *31*, L10501.
- Biomass ECV report (2009). Assessment of the status of the development of the standards for the Terrestrial Essential Climate Variables. 38–41.
- Boyd, D. S., Foody, G. M., & Curran, P. J. (1999). The relationship between the biomass of Cameroonian tropical forests and radiation reflected in middle infrared wavelengths (3.0–5.0  $\mu\text{m}$ ). *International Journal of Remote Sensing*, *20*, 1017–1023.
- Brown, S., Gillespie, A. J. R., & Lugo, A. E. (1989). Biomass estimation methods for tropical forests with applications to forest inventory data. *Forest Science Journal*, *35*, 881–902.
- Canadell, J. G., LeQu e, C., Raupach, M. R., Field, C. B., Buitenhuis, E. T., Ciais, P., Conway, T. J., Gillett, N. P., Houghton, R. A., & Marland, G. (2007). Contributions to accelerating atmospheric CO<sub>2</sub> growth from economic activity, carbon intensity, and efficiency of natural sinks. *Proceedings of the National Academy of Science of the United States of America*, *104*, 18866–18870. doi:10.1073/pnas.0702737104.
- Chacko, V. J. (1965). *A manual on sampling techniques for forest surveys*. Delhi: Manager of Publications.
- Champion, H. G., & Seth, S. K. (1968). *A revised survey of forest types of India*. New Delhi: Government of India Publication.
- Chavez, P. S. (1996). Image-based atmospheric corrections—revisited and improved. *Photogrammetric Engineering and Remote Sensing*, *62*, 1025–1036.
- Chen, S., & Rao, P. (2009). Regional land degradation mapping using MODIS data and decision tree (DT) classification in a transition zone between grassland and cropland of north-east China. In: Information Science and Engineering (ICISE), 2009 1st International Conference, Nanjing, China, 26–28th December 2009 (pp. 1395–1398). doi:10.1109/ICISE.2009.878.
- Chhabra, A., Palria, S., & Dadhwal, V. K. (2002). Growing stock-based forest biomass estimate for India. *Biomass and Bioenergy*, *22*, 187–194.
- Denman, K. L., Brasseur, G., Chidthaisong, A., Ciais, P., Cox, P. M., Dickinson, R. E., Hauglustaine, C., Heinze, E., Holland, D., Jacob, U., Lohmann, S., Ramachandran, P. L., DaSilva Dias, D., Wofsy, S. C., & Zhang, X. (2007). Couplings between changes in the climate system and biogeochemistry. In S. Solomon, D. Qin, M. Manning, Z. Chen, M. Marquis, K. B. Averyt, M. Tignorand, & H. L. Miller (Eds.), *Climate Change 2007* (pp. 541–584). Cambridge: Cambridge University Press.
- Dong, J., Kaufmann, R. K., Myneni, R. B., Tucker, C. J., Kauppi, P. E., Liski, J., Buermann, W., Alexeyev, V., & Hughes, M. K. (2003). Remote sensing estimates of boreal and temperate forest woody biomass: carbon pools, sources, and sinks. *Remote Sensing of Environment*, *84*, 393–410.
- Fearnside, P. M., & Laurance, W. F. (2003). Comment on ‘Determination of deforestation rates of the world’s humid tropical forests’. *Science*, *299*, 1015.
- Fearnside, P. M., & Laurance, W. F. (2004). Tropical deforestation and greenhouse gas emissions. *Ecological Applications*, *14*, 982–986.
- Food and Agricultural Organization of the United Nations (FAO). (2005). FAO Statistical database 2005. Source: <http://faostat.fao.org>.
- Foody, G. M., Cutler, M. E., McMorrow, J., Pelz, D., Tangki, H., Boyd, D. S., & Douglas, I. (2001). Mapping the biomass of Bornean tropical rain forest from remotely sensed data. *Global Ecology and Biogeography*, *10*, 379–387.
- Foody, G. M., Boyd, D. S., & Cutler, M. E. J. (2003). Predictive relations of tropical forest biomass from Landsat TM data and their transferability between regions. *Remote Sensing of Environment*, *85*, 463–474.
- Forest Survey of India (FSI). (2009). *State of forest report* (pp. 90–93). Dehradun: Ministry of Environment and Forests.
- Franklin, S. E., & Peddle, D. R. (1989). Spectral texture for improved class discrimination in complex terrain. *International Journal of Remote Sensing*, *10*, 1437–1443.
- Gibbs, H. K., Brown, S., Niles, J. O., & Foley, J. A. (2007). Monitoring and estimating tropical forest carbon stocks: making REDD a reality. *Environmental Research Letters*. doi:10.1088/1748-9326/2/4/045023. online access: [erl.iop.org](http://erl.iop.org).
- Hakkila, P. (1989). *Utilization of residual forest biomass*. Berlin: Springer.
- Hernandez, R. P., Koohafkan, P., & Antoine, J. (2004). Assessing carbon stocks and modelling win-win scenarios of carbon sequestration through land-use changes. FAO report. pp. 10–27.
- Houghton, R. A. (2005). Tropical deforestation as a source of greenhouse gas emissions. In P. Mutinho & S. Schwartzman (Eds.), *Tropical deforestation and climate change* (pp. 13–22). Belem: IPAM.
- Indian Council for Forestry Research and Education (ICFRE). (2007). *Views from ICFRE, Dehradun, India (an observer organization) to UNFCCC on REDD* (p. 5). Dehradun: ICFRE, Government of India.
- Intergovernmental Panel for Climate Change (IPCC). (2003). *Good practice guidance for land use land use change and forestry*. Hayama: IGES.
- Intergovernmental Panel on Climate Change (IPCC). (2006). Agriculture, forestry and other land use. In: H.S. Eggleston, L. Buendia, K. Miwa, T. Ngara, K. Tanabe (Eds.). IPCC Guidelines for National Greenhouse Gas Inventories. Prepared by the National Greenhouse Gas Inventories Programme. Japan: IGES. (<http://www.ipcc-nggip.iges.or.jp/public/2006gl/vol4.html>).
- Lillesand, T. M., Kiefer, R. W., & Chipman, J. W. (2007). *Remote sensing and image interpretation* (5th ed., pp. 491–624). Singapore: Wiley.
- Lu, D. (2005). Aboveground biomass estimation using Landsat TM data in the Brazilian Amazon. *International Journal of Remote Sensing*, *26*, 2509–2525.
- Lu, D. (2006). The potential and challenge of remote sensing-based biomass estimation. *International Journal of Remote Sensing*, *27*, 1297–1328.
- Lucas, R. M., Curran, P. J., Honzak, M., Foody, G. M., DoAmaral, I., & Amaral, S. (1998). The contribution of remotely sensed data in the assessment of the floristic composition, total biomass and structure of Amazonian tropical secondary forests. In C. Gascon & P. Moutinho (Eds.), *Regeneracao Florestal: Pesquisas na Amazonia* (pp. 61–82). Manaus: INPA.

- Luckman, A., Baker, J. R., Kuplich, T. M., Yanasse, C. C. F., & Frery, A. C. (1997). A study of the relationship between radar backscatter and regenerating forest biomass for space borne SAR instrument. *Remote Sensing of Environment*, *60*, 1–13.
- Luckman, A., Baker, J. R., Honzák, M., & Lucas, R. M. (1998). Tropical forest biomass density estimation using JERS-1 SAR: seasonal variation, confidence limits, and application to image mosaics. *Remote Sensing of Environment*, *63*, 126–139.
- Malhi, Y., & Grace, J. (2000). Tropical forests and atmospheric carbon dioxide. *Trends in Ecology & Evolution*, *15*, 332–337.
- Marceau, D. J., Howarth, P. J., Dubois, J. M., & Gratton, D. J. (1990). Evaluation of the grey-level co-occurrence matrix method for land-cover classification using SPOT imagery. *IEEE Transactions on Geoscience and Remote Sensing*, *28*, 513–519.
- Markham, B. L., & Barker, J. L. (1986). Landsat MSS and TM post-calibration dynamic ranges, exoatmospheric reflectances and at-satellite temperatures. *EOSAT Technical Notes*, *1*, 3–8.
- Ministry of Environment and Forests (MoEF). (2009). *Climate change negotiations: India's submissions to the United Nations Framework Convention on Climate Change* (p. 58). New Delhi: Government of India.
- Mund, M., Kummerow, E., Hein, M., Bauer, G. A., & Schulze, E. D. (2002). Growth and carbon stocks of a spruce forest chronosequence in central Europe. *Forest Ecology and Management*, *171*, 275–296.
- Nelson, R., Jimenez, J., Schnell, C. E., Hartshorn, G. S., Gregoire, T. G., & Oderwald, R. (2000). Canopy height models and airborne lasers to estimate forest biomass: two problems. *International Journal of Remote Sensing*, *21*, 2153–2162.
- Pandya, M. R., Singh, R. P., Murali, K. R., Babu, P. N., Kirankumar, A. S., & Dadhwal, V. K. (2002). Bandpass solar exo-atmospheric irradiance and Rayleigh optical thickness of sensors onboard Indian Remote Sensing satellites-1B, 1C, 1D and P4. *IEEE Transactions on Geoscience and Remote Sensing*, *40*, 714–718.
- Phua, M. H., & Saito, H. (2003). Estimation of biomass of a mountainous tropical forest using Landsat TM data. *Canadian Journal of Remote Sensing*, *29*, 429–440.
- Plugge, D., Baldauf, T., Ratsimba, H. R., Rajoelison, G., & Köhl, M. (2010). Combined biomass inventory in the scope of REDD (Reducing Emissions from Deforestation and Forest Degradation). *Madagascar Conservation and Development*, *5*, 23–34.
- Podest, E., & Saatchi, S. (2002). Application of multiscale texture in classifying JERS-1 radar data over tropical vegetation. *International Journal of Remote Sensing*, *23*, 1487–1506.
- Popescu, S. C., Wynne, R. H., & Nelson, R. F. (2003). Measuring individual tree crown diameter with lidar and assessing its influence on estimating forest volume and biomass. *Canadian Journal of Remote Sensing*, *29*, 564–577.
- Ravindranath, N. H., & Ostwald, M. (2008). Carbon inventory methods: handbook for greenhouse gas inventory, carbon mitigation and roundwood production projects (pp. 41–44, 181–199). Heidelberg: Springer.
- Riedel, T. (2008). Evaluierung alternative Stichprobenkonzepte für die Bundeswaldinventur. Unpublished Ph.D. dissertation. Department Biologie der Fakultät für Mathematik, Informatik und Naturwissenschaften. Universität Hamburg.
- Rignot, E. J., Zimmermann, R., & van Zyl, J. J. (1995). Spaceborne applications of P band imaging radars for measuring forest biomass. *IEEE Transactions on Geoscience and Remote Sensing*, *33*, 1162–1169.
- Roy, P. S., & Ravan, S. A. (1996). Biomass estimation using satellite remote sensing data—an investigation on possible approaches for natural forest. *Journal of Biosciences*, *21*, 535–561.
- Sader, S. A., Waide, R. B., Lawrence, W. T., & Joyce, A. T. (1989). Tropical forest biomass and successional age class relationships to a vegetation index derived from Landsat TM data. *Remote Sensing of Environment*, *28*, 143–156.
- Santos, J. R., Lacruz, M. S. P., Araujo, L. S., & Keil, M. (2002). Savanna and tropical rainforest biomass estimation and spatialization using JERS-1 data. *International Journal of Remote Sensing*, *23*, 1217–1229.
- Santos, J. R., Freitas, C. C., Araujo, L. S., Dutra, L. V., Mura, J. C., Gama, F. F., Soler, L. S., & Sant' Anna, S. J. S. (2003). Airborne P-band SAR applied to the aboveground biomass studies in the Brazilian tropical rainforest. *Remote Sensing of Environment*, *87*, 482–493.
- Schulze, E. D. (2000). *Carbon and nitrogen cycling in European forest ecosystems*. Heidelberg: Springer.
- Sharma, R. K., Lall, P., & Hofstad, O. (2008). Forest biomass density, utilization and production dynamics in a western Himalayan watershed. *Journal of Forestry Research*, *19*, 171–180.
- Sharma, L. K., Pandey, P. C., & Nathawat, M. S. (2012). Assessment of land consumption rate with urban dynamics change using geospatial techniques. *Journal of Land Use Science*, *7*, 135–148.
- Sinha, S., Sharma, L. K., & Nathawat, M. S. (2012). Tigers losing grounds: impact of anthropogenic occupancy on tiger habitat suitability using integrated geospatial-fuzzy techniques. *The Ecoscan*, *1*, 259–263.
- Sobrino, J. A., Jiménez-Muñoz, J. C., & Paolini, L. (2004). Land surface temperature retrieval from LANDSAT TM 5. *Remote Sensing of Environment*, *90*, 434–440.
- Steininger, M. K. (2000). Satellite estimation of tropical secondary forest aboveground biomass data from Brazil and Bolivia. *International Journal of Remote Sensing*, *21*, 1139–1157.
- Stephens, B. S., et al. (2007). Weak Northern and strong tropical land carbon uptake from vertical profiles of atmospheric CO<sub>2</sub>. *Science*, *316*, 1732–1735.
- Trigg, S. N., Curran, L. M., & McDonald, A. K. (2006). Utility of Landsat 7 satellite data for continued monitoring of forest cover change in protected areas in southeast Asia. *Singapore Journal of Tropical Geography*, *27*, 49–66.
- United Nations Framework Convention on Climate Change (UNFCCC) (1998, 2006). Kyoto Protocol to the United Nations Framework Convention on Climate Change. United Nations. Source: <http://unfccc.int>.
- van der Meer, F. (1996). Spectral mixture modeling and spectral stratigraphy in carbonate lithofacies mapping. *ISPRS Journal of Photogrammetry and Remote Sensing*, *51*, 150–162.
- van der Werf, G. R., Morton, D. C., DeFries, R. S., Olivier, J. G. J., Kasibhatla, P. S., Jackson, R. B., Collatz, G. J., & Randerson,



- J. T. (2009). CO<sub>2</sub> emissions from forest loss. *Nature Geoscience*, 2, 737–738.
- Wirth, C., Czimczik, C. I., & Schulze, E. D. (2002). Beyond annual budgets: carbon flux at different temporal scales in fire-prone Siberian Scots pine forests. *Tellus*, 54B, 611–630.
- Wirth, C., Schumacher, J., & Schulze, E. (2004). Generic biomass functions for Norway spruce in Central Europe—a meta-analysis approach toward prediction and uncertainty estimation. *Tree Physiology*, 24, 121–139.
- Woodcock, C. E., Collins, J. B., Jakabhazy, V. D., Li, X., Macomber, S., & Wu, Y. (1997). Inversion of the Li–Strahler canopy reflectance model for mapping forest structure. *IEEE Transactions on Geoscience and Remote Sensing*, 35, 405–414.
- Zheng, D., Rademacher, J., Chen, J., Crow, T., Bresee, M., Moine, J. L., & Ryu, R. (2004). Estimating aboveground biomass using Landsat 7 ETM+ data across a managed landscape in northern Wisconsin, USA. *Remote Sensing of Environment*, 93, 402–411.